Detailed FT near-infrared study of the behaviour of water and hydroxyl in sedimentary length-fast chalcedony, SiO$_2$, upon heat treatment

Patrick Schmidt*, Aïcha Badou, François Fröhlich

Muséum national d'histoire naturelle, Dpt. de Préhistoire UMR 7194, Centre de spectroscopie infrarouge CP 57, 57, rue Cuvier 75231, Paris Cedex 05, France

ABSTRACT

Chalcedony is a porous spatial arrangement of hydroxylated nanometre sized α-quartz (SiO$_2$) crystallites. Due to micro-structural transformations upon heat treatment, the optical and mechanical properties of the rock are modified. We investigated these transformations in sedimentary length-fast chalcedony through Fourier Transform near- and mid-infrared spectroscopy using direct transmission and the reflectivity. Chemical adsorption potential and absorption of H$_2$O by pores was studied after heat treatment. We found that water held in open porosity is reduced upon heat treatment to temperatures above 150 °C. Silanole is noticeably lost from 250 to 300 °C upwards and new bridging Si–O–Si further reduces the surface of open pores, creating a less porous material. Molecular water, resulting from the reaction Si–OH HO–Si → Si–O–Si + H$_2$O creates new isolated pores within the material. At temperatures above 500 °C, the samples start internal fracturing, permitting water held in isolated pores to be evacuated. These results shed light on thermal transformations in chalcedony and allow for a better understanding of mechanical transformations after heat treatment.

1. Introduction

Chalcedony consists of a spatial arrangement of 50–100 nm measuring α-quartz crystallites [1]. The crystallites align in fibres ranging up to several millimetres or even centimetres in well crystallised specimens. Based on orientation of the crystallites within these fibres, several authors have distinguished different types of chalcedony [2–4]. The most common type in nature is length-fast chalcedony with an orientation of the quartz *c*-axis perpendicular to the fibre axis (referred to as chalcedony hereafter) [2]. Flint typically consists of length-fast chalcedony with shorter and somewhat less organised fibres that are not easy to discern under the polarised light microscope. Crystallographic studies have shown that the crystallites forming chalcedony fibres are polysynthetic twins according to the Brazil law on a very small scale [3,5]. Studies concerning the water content of chalcedony [6–9] show up to 2 wt% of total water. These works subdivide the total water content into molecular water H$_2$O and silanole SiOH. Molecular water in chalcedony is mainly adsorbed in pores and interstices [6], a part of which may be interconnected to form a network of open or closed porosity. The crystallite surface at the walls of open pores is covered with silanole, forming hydrogen bonds (H-bonds) with each other and with molecular water held in the vicinity of the grain boundaries [7]. Twin interfaces are another

site where surface silanole can be expected [7]. A third type of hydroxyl is structural silanole that compensates free charges due to impurities and defects in the quartz lattice [8]. The concentration of structural silanole, however, was shown to be insignificant in chalcedony [6]. Due to the strong polar nature of the OH bond, infrared spectroscopy is a convenient and frequently used means of studying water related defects in quartz and chalcedony [8,10–13]. Fundamental vibrations of silanole and molecular water cause a broad absorption in the mid infrared at ≈3400 cm^{-1} that interferes with the OH stretching vibration of silanole [8,11]. The SiOH combination mode, involving O–H stretching and Si–O–H bending, causes a band in the near-infrared (NIR) between 4600 and 4300 cm^{-1} [14]. H$_2$O is individualised through a ($\nu_2 + \nu_3$) combination band around 5200 cm^{-1} and the first overtone of the stretching vibration at 7000 cm^{-1} [14,15]. The shapes of the combination bands of water and silanole are sensitive to hydrogen bonding. The SiOH absorption shifts to lower wavenumbers when silanole is involved in H-bonding with neighbouring silanoles or molecular water [6,7,15]. Langer and Flörke [15] identified two types of SiOH in opals and showed the combination band to be a convolution of a high energy component, free from H-bonding, and a low energy component, representing hydrogen bonded silanole. The fundamental OH stretching vibration frequency is also sensitive to hydrogen bonding and the band shifts between 3750 cm^{-1} for isolated- and 3500 cm^{-1} for strongly H-bonded groups [16–18]. Isolated SiOH in chalcedony, not or almost not involved in hydrogen bonding, can be measured through an OH stretching band at 3740 cm^{-1} [7,8,17,19].

* Corresponding author. Tel.: +33 634281896.
  E-mail address: schmidt@mnhn.fr (P. Schmidt).

Table 1
Samples, description and thicknesses (C = concentration before annealing as determined by the NIR absorption in the hydrated state).

Sample	Description	No. of samples	Thickness	C SiOH [wt%]	C H$_2$O [wt%]
SB-Cal-07	Length-fast chalcedony from an agate geode.	7	670 ± 10 μm	0.31	0.61
SB-Cal-06	Length-fast chalcedony from an agate geode.	1	720 ± 10 μm	0.32	0.56
PS-S-02	Turonian fine flint, consisting of length-fast chalcedony. East of Tours, France.	2	705 ± 5 μm	0.50	0.66
PS-09-04	Coniacian black flint, Étretat, France.	1	545 ± 5 μm	0.58	0.73
PS-09-07	Santonian grey flint from dedolomised chalk level, cliffs of Étretat, France.	1	1037 ± 5 μm	0.45	0.45
PS-09-11	Turonian black flint, cliffs of Étretat, France.	1	997 ± 5 μm	0.63	0.56
PS-09-13	Turonian black flint with grey cortex, cliffs of Étretat, France.	1	556 ± 5 μm	0.6	0.59
PS-09-14	Turonian black flint, cliffs of Étretat, France.	1	538 ± 5 μm	0.5	0.71
PS-09-15	Turonian brown flint, north of *Le grand Pressigny*, France.	1	982 ± 5 μm	0.75	0.75
PS-09-24	Turonian brown to ochre flint, *Le grand Pressigny*, France.	1	995 ± 5 μm	0.55	0.61
PS-09-25	Upper Cretaceous brown flint, *Le grand Pressigny*, France.	1	998 ± 5 μm	0.72	0.74
PS-09-38	Upper Cretaceous light grey flint containing lutécite. From detritic sand deposit, north of *Le grand Pressigny*, France.	1	1050 ± 5 μm	0.6	0.73
PS-09-41	Turonian brown to ochre flint, *Le grand Pressigny*, France.	1	549 ± 5 μm	0.61	0.67

In a previous study, Schmidt and Fröhlich [20] showed that the thermal evolution of the mid infrared absorption band at 555 cm^{-1} can be used for evaluating the formation of new bridging Si–O–Si after the evacuation of Si–OH from chalcedony. The disappearance of the band at temperature above 300 °C is due to recrystallisation resulting from heat treatment.

Based on the infrared signature of water in chalcedony, we present here new data on the process of 'dehydration' of chalcedony upon heat treatment. The work was undertaken in order to shed light on micro-structural transformations when the rock is subjected to heat treatment. The study gives new insight into thermal response, structural changes at the crystallite boundaries and the evolution of porosity.

2. Samples and experimental

11 samples of flint from different origins in the Paris Basin (France), all consisting of sedimentary length-fast chalcedony, and two samples of agate of unknown provenience, consisting of hydrothermal length-fast chalcedony, were analysed. Sample numbers and descriptions are resumed in Table 1. All samples were cut into sections with thicknesses between 600 and

1100 μm and diamond polished on both sides. The transmission was measured at normal incidence between 5600 and 3000 cm^{-1} with a resolution of 8 cm^{-1}, using a Brucker Vector 22 FTIR spectrometer and unpolarised radiation. A circular aperture of 12 mm diameter delimited the analysed area on the slabs. The baseline for absorbance measurements of the two combination bands was a straight line between the two lowest points on either side of the absorption bands (Fig. 1a). The baseline for the absorbance measurements of isolated SiOH at 3740 cm^{-1} is shown in Fig. 1b. Error bars for the measured absorptions were calculated by repeating spectral acquisition 30 times on one sample.

The quantitative determination of the silanole and molecular water contents was calculated, using the molar absorption coefficients given by Scholze [14]. H$_2$O concentration was determined through the linear absorption coefficient α = 1.14 L/mol cm, measured at 5430 cm^{-1}. Due to morphology changes of the SiOH combination band upon heat treatment, the silanole concentration was calculated with the integral absorption coefficient α = 160 L/mol cm^2.

Mid infrared reflectance data at 555 cm^{-1} was collected on the polished surfaces of the 11 flint samples. Spectra were obtained between 600 cm^{-1} and 400 cm^{-1} with a resolution of 2 cm^{-1} on the
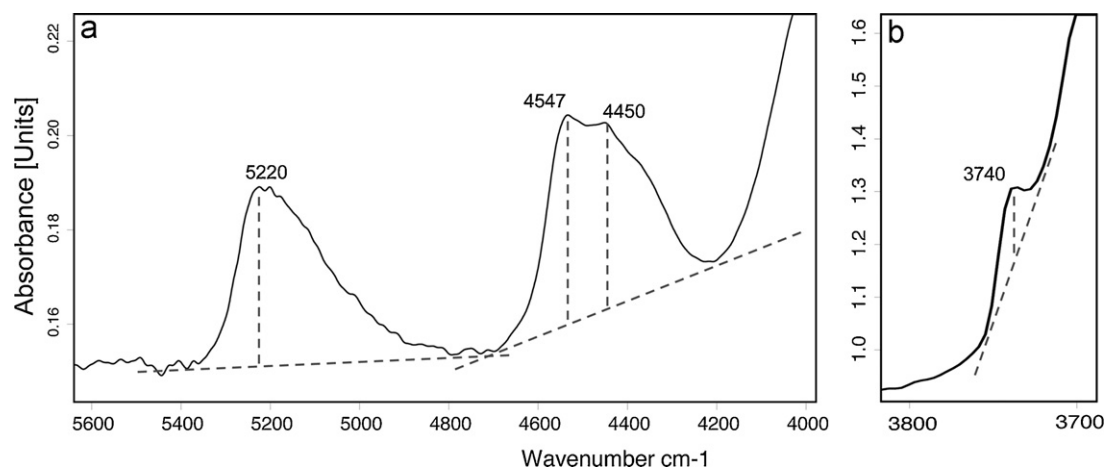

Fig. 1. Baselines used for the measurement of the absorbances that are referred to in the text.

same spectrometer. The reflection coefficient (R) was measured at 45° with unpolarised radiation.

All samples underwent heat treatment in order to assess the thermal evolution of the different OH species. The annealing sequence was as follows. The samples were dehydrated at 110 °C for 48 h in an electrical furnace. Spectra were recorded in the dry state immediately after the samples had cooled to room temperature. The samples were then rehydrated in deionised H_2O for one night and a second spectrum was acquired in the hydrated state. After this, the samples were heated to 150 °C for 6 h and the transmission was measured in the dry state immediately after the samples had cooled to room temperature. The samples were rehydrated in deionised H_2O for one night and the transmission was measured in the rehydrated state. The samples were then heated to the next higher temperature and the measuring protocol was repeated. This sequence was continued with 50 °C steps until 600 °C. The annealing temperatures were held for 6 h. Ramp rates for each temperature step were chosen in order to prevent fracturing of the slabs. Rates varied from 20 °C/min for the low temperature steps and 0.2 °C/min for the 600 °C heating step. All transmission measurements were acquired at room temperature.

In order to verify if this experimental protocol is representative of samples that are heated to a single temperature, the sample SB-Cal-07 was cut into 7 slabs. Two of these polished sections underwent the complete sequence and the 5 remaining sections were heated to single temperatures (350 °C, 400 °C, 450 °C, 500 °C and 550 °C) for control. These control samples permit to evaluate the difference between the heating of a single sample to successive temperatures and a sample heated to a single temperature. Additionally, two sections from samples SB-Cal-07 and PS-S-02 respectively underwent the complete annealing sequence but were held at the maximum temperature for different durations (3 h and 6 h). If the observed changes in the spectra are due to the

maximum temperature of the heat treatment or the total time of annealing can be seen by the comparison between these control samples.

Due to technical problems, the samples heated to 200 °C could not be analysed immediately after they had cooled to room temperature. Samples had time (approx. 30 min) to adsorb small amounts of H_2O from atmospheric humidity and yielded spectra of slightly rehydrated samples. The dehydrated state data for the 200 °C heating step is therefore missing. This experience shows the difficulty to maintain chalcedony samples in a dehydrated state after heat treatment.

3. Results

3.1. NIR spectra

Spectra of all samples show the expected SiOH combination band near 4500 cm^{-1} and the H_2O combination band near 5220 cm^{-1}. The sample's molecular water and silanole contents before annealing are: 0.59–0.75 wt% H_2O and 0.45–0.75 wt% SiOH. Upon heat treatment the samples show temperature dependent evolution of the two bands.

3.1.1. Hydroxyl loss upon heat treatment
3.1.1.1. Silanoles. The near infrared spectra of samples annealed to successive temperatures show the loss of silanole upon heat treatment. Fig. 2 shows the reduction of silanole, measured at 4547 cm^{-1}, as a function of temperature for flint (Fig. 2a–c) and agate samples (Fig. 2d). The values plotted in Fig. 2 are extracted from spectra acquired on samples in their dehydrated state. The graphs show the silanole content of the samples to remain stable until 250 °C within the limits of the calculated error. The silanole content is progressively reduced at temperatures higher than 300 °C. The rate of decrease slows down at approximately
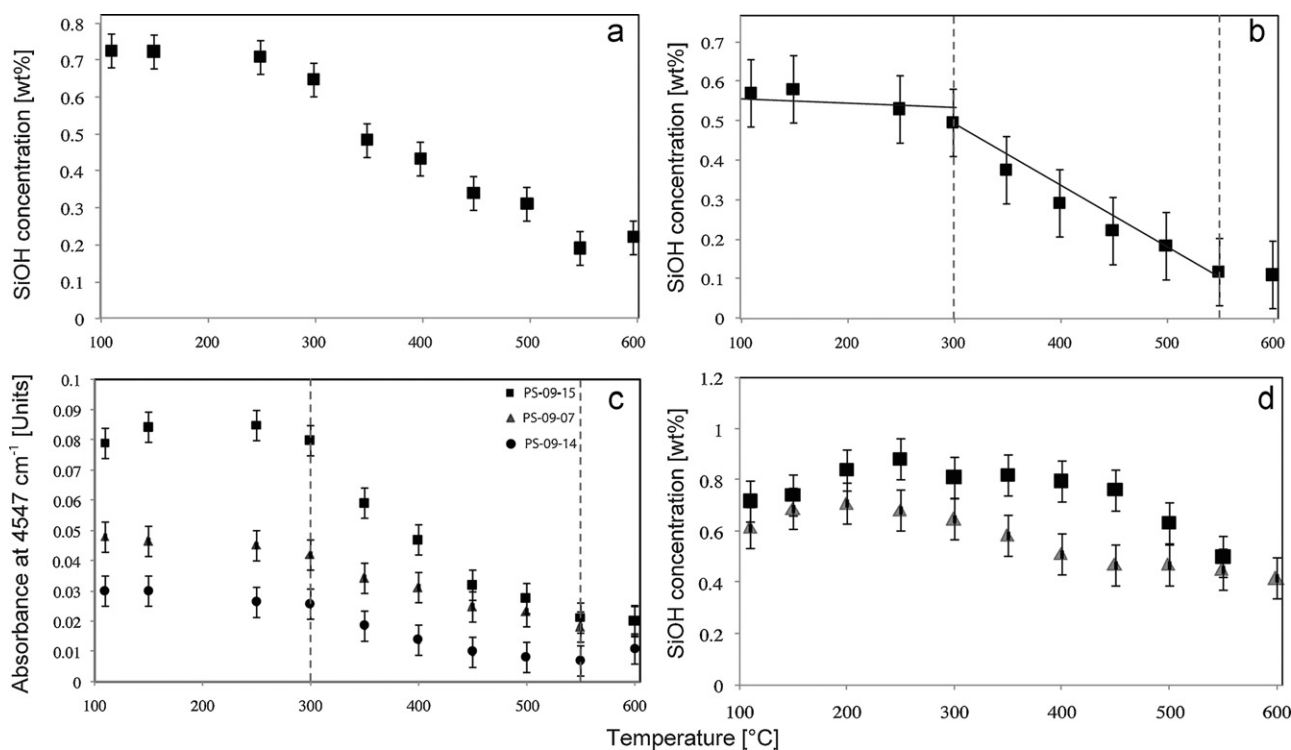

Fig. 2. Plots showing the reduction of SiOH in dehydrated flint and agate samples. The concentration of SiOH in wt% as calculated from the absorbance at 4547 cm^{-1} in the spectra, acquired on dehydrated samples, is plotted against the annealing temperature the samples were heat treated at: (a) PS-09-25, (b) PS-09-04, the dotted lines mark the 3 observed intervals (see Section 3.1.1). (d) Agate samples SB-Cal-06 (squares ■) and Sb-Cal-07 (triangles ▲), showing a different pace of SiOH loss upon heat treatment. (c) Plot of the values of absorbance at 4547 cm^{-1} in dehydrated state spectra of PS-09-14/15/07, showing the 3 temperature intervals that are found in all flint samples.
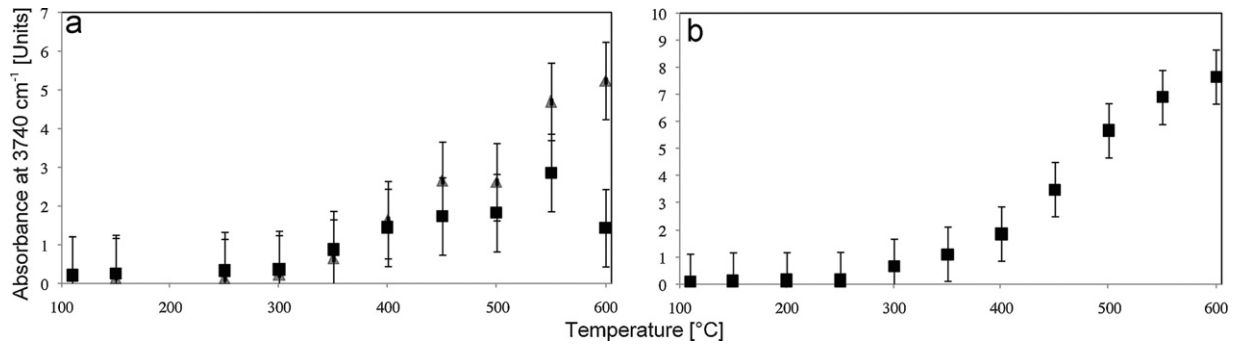
Fig. 3. Plots of the value of absorbance of the fundamental OH stretching vibration at 3740 cm^{-1} against the annealing temperature in dehydrated state spectra. (a) Flint samples PS-09-07 (■), PS-09-41 (▲). (b) Agate sample SB-Cal-07. The plots show that SiOH becomes more isolated from 300 °C upwards.

550 °C and the curves become flatter. These curves indicate the presence of three temperature intervals, (1) until 250–300 °C, (2) between 300 °C and 550 °C and (3) above 550 °C. The majority of the loss of silanole takes place between 300 °C and 550 °C. The observed three intervals are found in all 11 flint samples. The plot of the integrated total area under the combination band as a function of temperature (Fig. 6a) shows the same three intervals. The agate samples show a somewhat different evolution of SiOH (Fig. 2d). Silanole is lost in these samples from 200 °C to 250 °C upwards but the three temperature intervals seen in flint are not observed.

The plots of the intensity of the fundamental OH stretching band of isolated SiOH groups at 3740 cm^{-1} (Fig. 3) show the increase of silanole not involved in hydrogen bonding. The values are extracted from spectra in the dehydrated state. The concentration of isolated SiOH increases from 300 °C upward in the flint (Fig. 3a) and agate samples (Fig. 3b). However, in 3 flint samples the isolation of SiOH

begins at higher temperatures ≈ 500 °C. These 3 samples also show a gain of molecular water upon heating.

3.1.1.2. Molecular water. No homogenous thermal evolution of the H$_2$O band at 5220 cm^{-1} is observed in the dehydrated state spectra of the 11 flint samples. In dehydrated samples this band expresses the concentration of water strongly retained in closed pores or interstices that cannot be easily evacuated. The band shows a gain of molecular water from 300 °C upwards for 3 samples (Fig. 4a, these 3 samples are the ones showing the isolation of SiOH at 500 °C) and the loss of almost all H$_2$O for 2 samples (Fig. 4b). The remaining flint samples show H$_2$O to increase between 250–300 °C and 400–500 °C and to be lost above this temperature (Fig. 4c). This heterogeneity might be correlated to internal fracturing (macroscopically observed on the samples) which was very heterogeneous in the 11 flint samples. Some samples did not crack until 600 °C
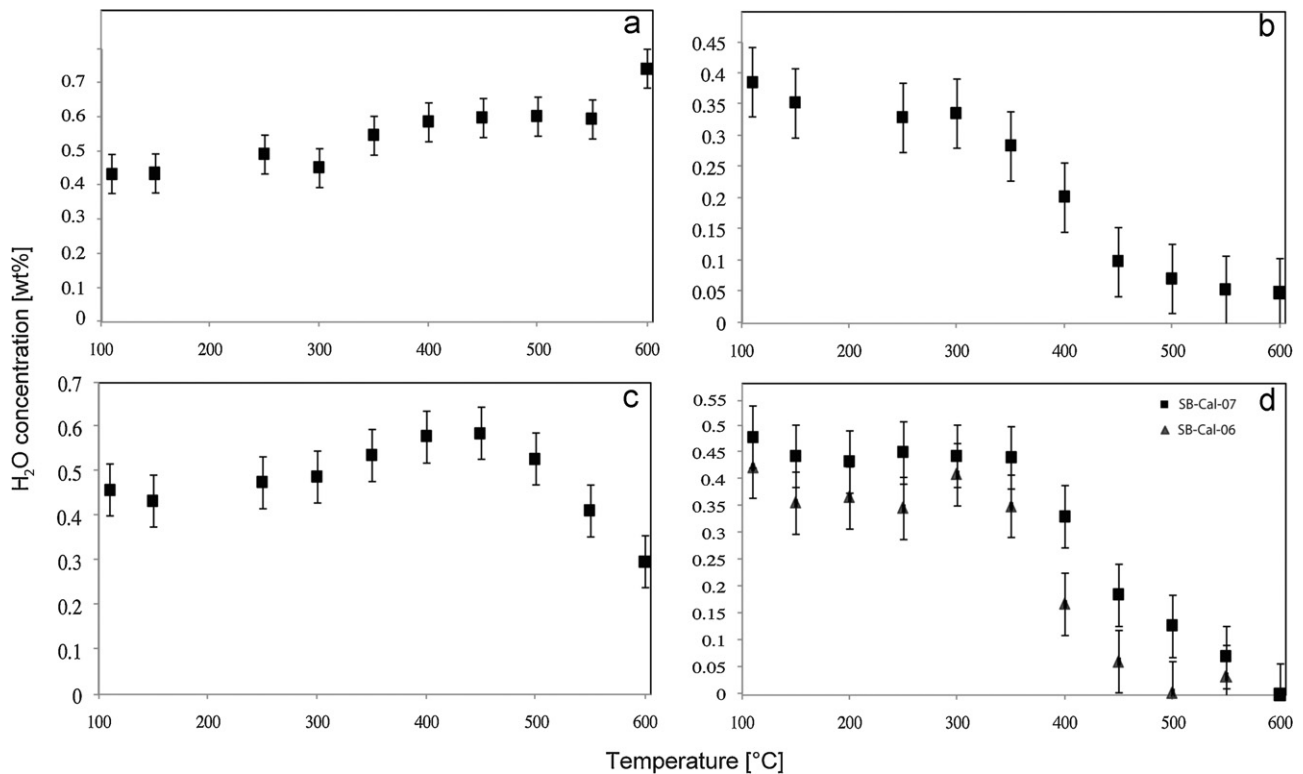

Fig. 4. Plots of the concentration of H$_2$O in wt% as measured by the absorbance of the combination band at 5220 cm^{-1} against the annealing temperature of flint and agate samples in the dehydrated state. The plots show the loss/gain of H$_2$O as a function of temperature. (a) PS-09-14, the concentration of molecular water is augmented. This graph is representative of 3 flint samples. (b) PS-09-41, H$_2$O is lost from 300 °C upwards. This graph is representative of 2 flint samples. (c) PS-09-13, H$_2$O augments until a temperature between 400 °C and 500 °C and is lost at higher temperatures. This graph is representative of 6 flint samples. (d) Two agate samples, H$_2$O is continuously lost from 300 °C upwards.
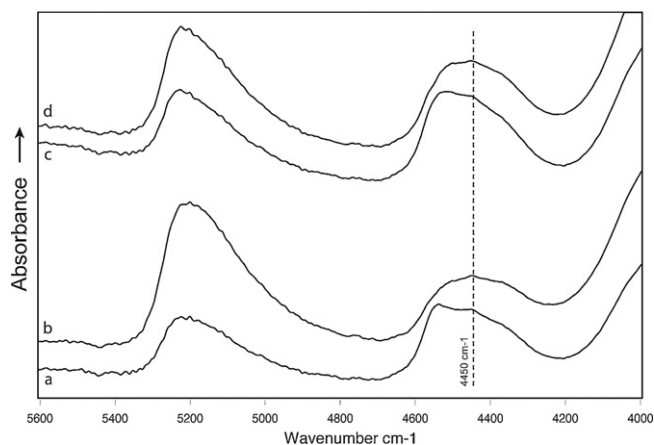
Fig. 5. Room temperature NIR spectra of the OH region of flint sample PS-S-02 (top) and agate sample SB-Cal-07 (bottom). (a) SB-Cal-07 dehydrated spectrum; (b) hydrated; (c) PS-S-02 dehydrated spectrum; (d) hydrated. The H_2O band near 5220 cm^{-1} is more intense in the hydrated state. The SiOH band near 4540 cm^{-1} is shaper in the dehydrated state. Spectra displaced vertically and acquired at room temperature.

whereas others turned completely white due to internal fractures. Two of the samples showed almost no fracturing (PS-09-38/41). The H_2O content of these samples decreases constantly from 300 °C upwards (Fig. 4b). The two agate samples were also free from fracturing until 600 °C. The plot of their H_2O content shows continuous loss of water from 350 °C upwards (Fig. 4d). The 3 samples that gain water over the total temperature interval (Fig. 4a) also show little internal fracturing. The intensity of internal fracturing of the samples might be correlated with the curves showing their H_2O loss. However, the numerical size of the studied sample does not seem to be sufficient for ascertaining such a correlation.

3.1.2. Comparison between spectra of hydrated an dehydrated samples

Fig. 5 shows spectra of a flint (top) and an agate sample (bottom) in their hydrated (b, d) and dehydrated (a, c) states. The H_2O band is more intense in the hydrated state spectra. The shape of the SiOH band varies between dehydrated and hydrated states, indicating a different involvement of the silanole content in H-bonding. The band is sharper in the spectra of dehydrated samples (Fig. 5) and the integrated total area under it is larger (Fig. 6a). The larger area under the band in dehydrated state spectra suggests that the molar absorption coefficient of the SiOH combination band is higher in the absence of H-bonding. Exact quantitative determinations of silanole in chalcedony must take into account the differences between molar absorption coefficients in both states, creating the need for a dehydrated state coefficient. The summit of the band lies at 4547 cm^{-1} for dehydrated state spectra whereas it is located at 4450 cm^{-1} in hydrated state spectra. When dehydrated samples are hydrated, the band's summit shifts back to a lower wavenumber, indicating that silanole can form new H-bonds with H_2O in open porosity. Fig. 6b–d shows three representative examples of the ratio between the values of absorbance at 4547 cm^{-1} and 4450 cm^{-1} plotted against the annealing temperature in the spectra of the hydrated samples. This ratio is a measure of the shape of the combination band in the hydrated state and therefore the state of involvement of SiOH in H-bonding. A value <1 indicates that the summit of the band is located at 4547 cm^{-1}, a value >1 at 4450 cm^{-1}. This ratio is close to 0.8 for samples heated to temperature less than 300 °C. The temperature at which the ratio shifts above unity lies at 350 °C for the 11 flint samples (Fig. 6b and c) and 400 °C for the agate samples (Fig. 6d). This temperature lies 50–100 °C higher than the temperature at which the samples begin to lose silanole. Once the ratio >1, the band does not shift back to a lower frequency when it is rehydrated. The SiOH combination band of rehydrated samples that were heated to temperatures
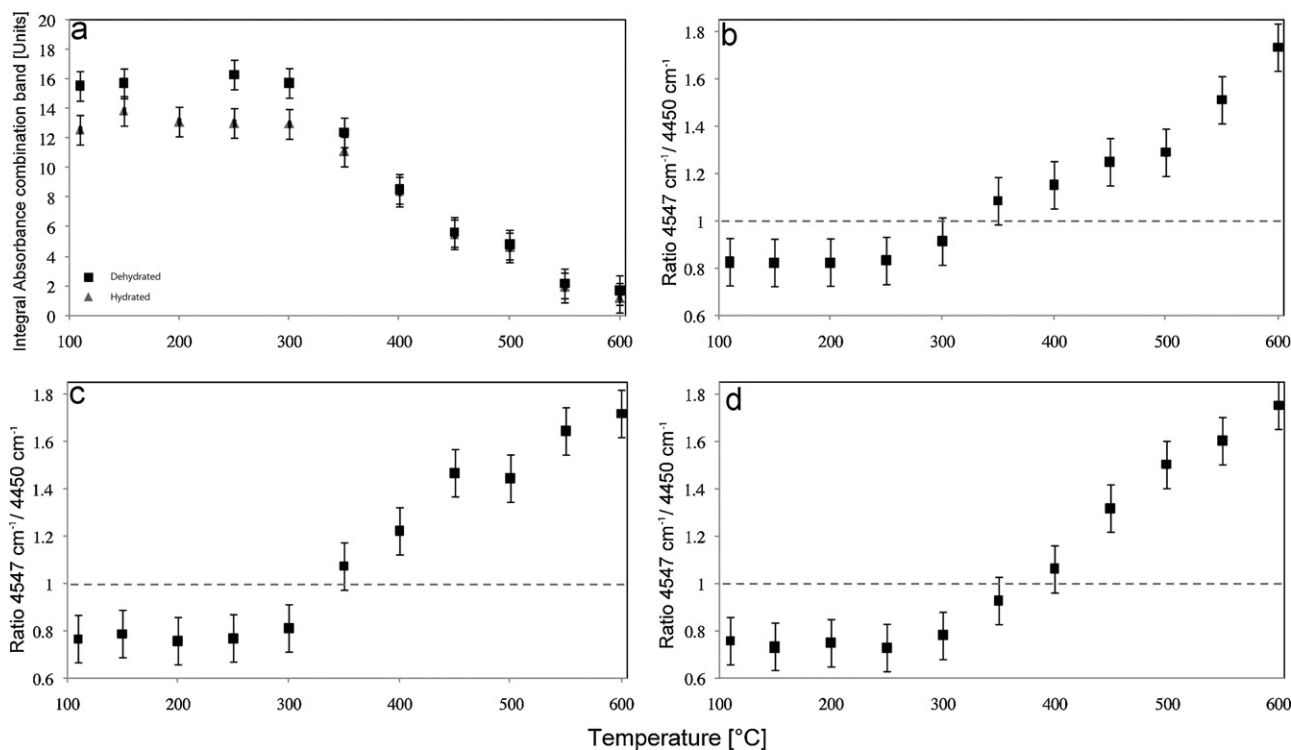

Fig. 6. (a) Plot of the value of the integrated total area under the SiOH combination band near 4540 cm^{-1} plotted against temperature of heat treatment for PS-09-24 in the hydrated (▲) and dehydrated (■) state. The plot shows the area to be larger in the dehydrated state spectra when they are heated to temperatures below 300 °C. There is no difference in the area in samples heated to temperatures above 300 °C. (b) and (c) Ratio between the absorbance at 4547 cm^{-1}/4450 cm^{-1} plotted against annealing temperature. (b) PS-09-15; (c) PS-09-38 Hydrated state spectra. The ratio increases from 300 °C upward. (d) 4547 cm^{-1}/4450 cm^{-1} ratio for agate sample SB-Cal-07.
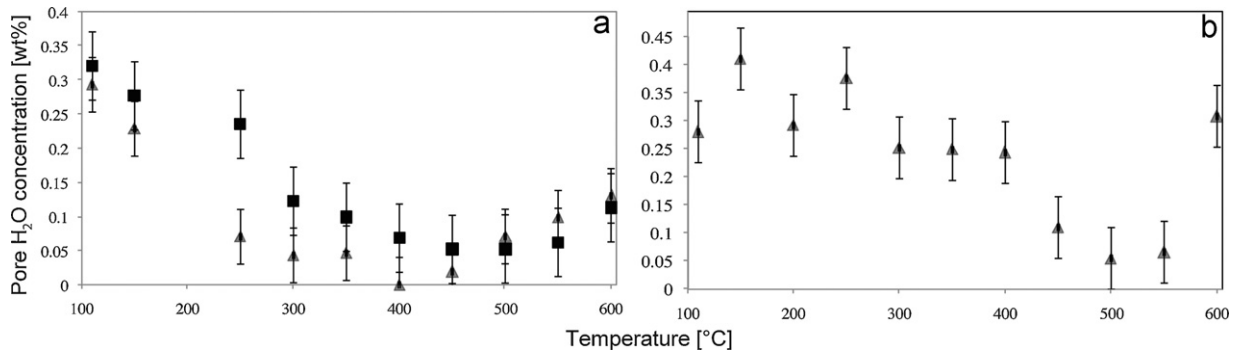
Fig. 7. Plots of the concentration of open porosity H_2O after heat treatment plotted against annealing temperature. The values are obtained by subtracting the intensity of the H_2O band in the dehydrated state spectra from the intensity of the band in the hydrated state spectra. (a) PS-09-25 (■) and -04 (▲). The plots are representative for the 11 flint samples. (b) Agate sample SB-Cal-07.
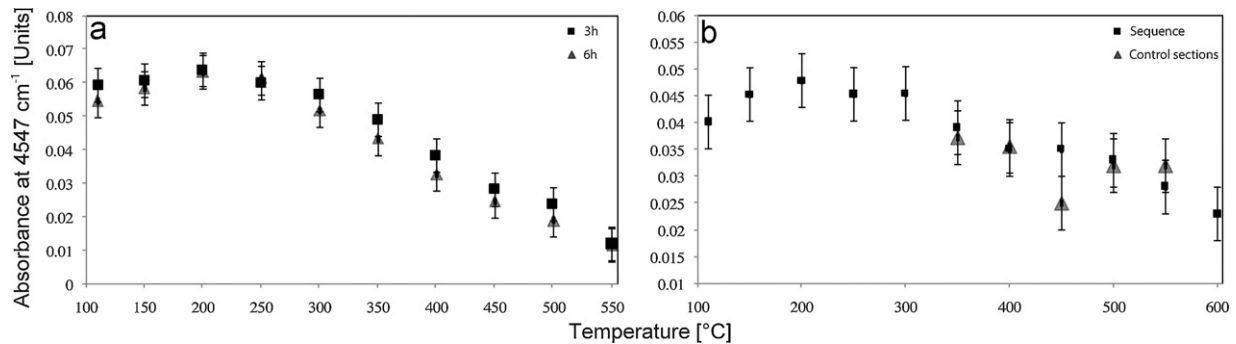

Fig. 8. Plots showing the reduction of SiOH in dehydrated flint and agate samples. (a) PS-S-02: comparison between two heating sequences where the annealing temperatures were held during 3 h and 6 h, respectively. (b) Comparison between the SiOH loss in a section of SB-Cal-07 that underwent the complete heating sequence and the control samples. For explanation see Section 2.

above $\approx 300\,°C$ is identical in shape with the band in the dehydrated state (Fig. 6a) showing that silanole cannot form H-bonds with H_2O in the open porosity of the samples.

The difference between the value of absorbance of the $5220\,cm^{-1}$ H_2O band in the dehydrated state spectra and its value in the hydrated state spectra is proportional to the amount of molecular water [6] that is held in open porosity (H_2O_{pores}) of the samples. Fig. 7 shows the content of open porosity H_2O after heat treatment and subsequent rehydration, plotted against annealing temperature. The flint samples show constant decrease of the quantity of H_2O_{pores} from $150\,°C$ until $400\,°C$ to $550\,°C$ and an increase above this temperature (Fig. 7a). The turning point lies at higher temperatures in agate samples (Fig. 7b) and flint samples with little internal fractures. This turning point between (1) decrease of H_2O_{pores} and (2) increase corresponds to the temperature at which the samples

exhibit the beginning of internal fracturing determined in macroscopic observations of the sections.

3.1.3. Assessment of the validity of the experimental protocol

The amount of silanole lost during heat treatment is the same for sections heated during 3 h and 6 h (Fig. 8a). The 5 control sections of SB-Cal-07, each heated to a different temperature, lost the same amount of silanole as the section that underwent the complete sequence (Fig. 8b).

The $4547\,cm^{-1}/4450\,cm^{-1}$ ratio of samples heated during 3 h and 6 h are identical throughout the complete annealing sequence within the limits of the calculated error (Fig. 9a). Three of the 5 control sections of SB-Cal-07, each heated to a different temperature, show the ratio to be the same as in the section that underwent the
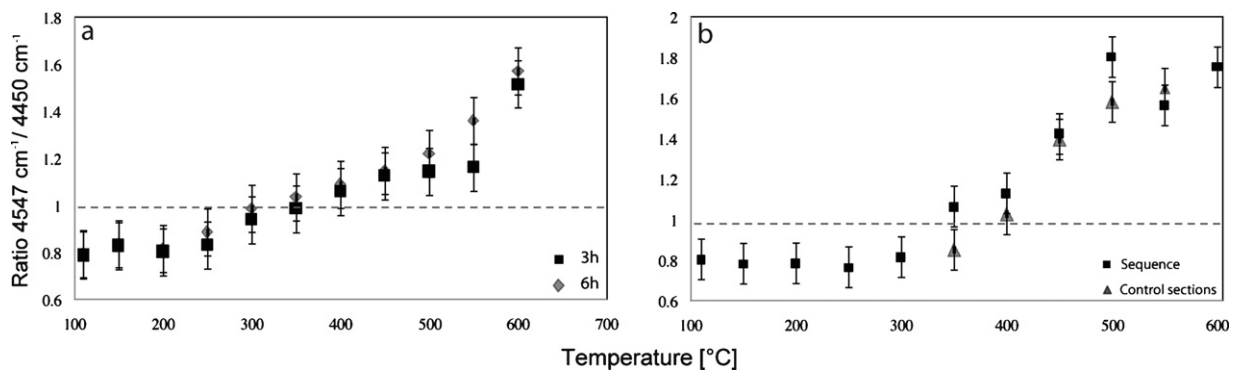

Fig. 9. (a) Plots of the ratio between the absorbance at $4547\,cm^{-1}/4450\,cm^{-1}$ against annealing temperature for PS-S-02 held at the annealing temperatures during 3 h and 6 h. (b) Plots of the same ratio for a section of SB-Cal-07 that underwent the complete heating sequence and the control samples. For explanation see Section 2.
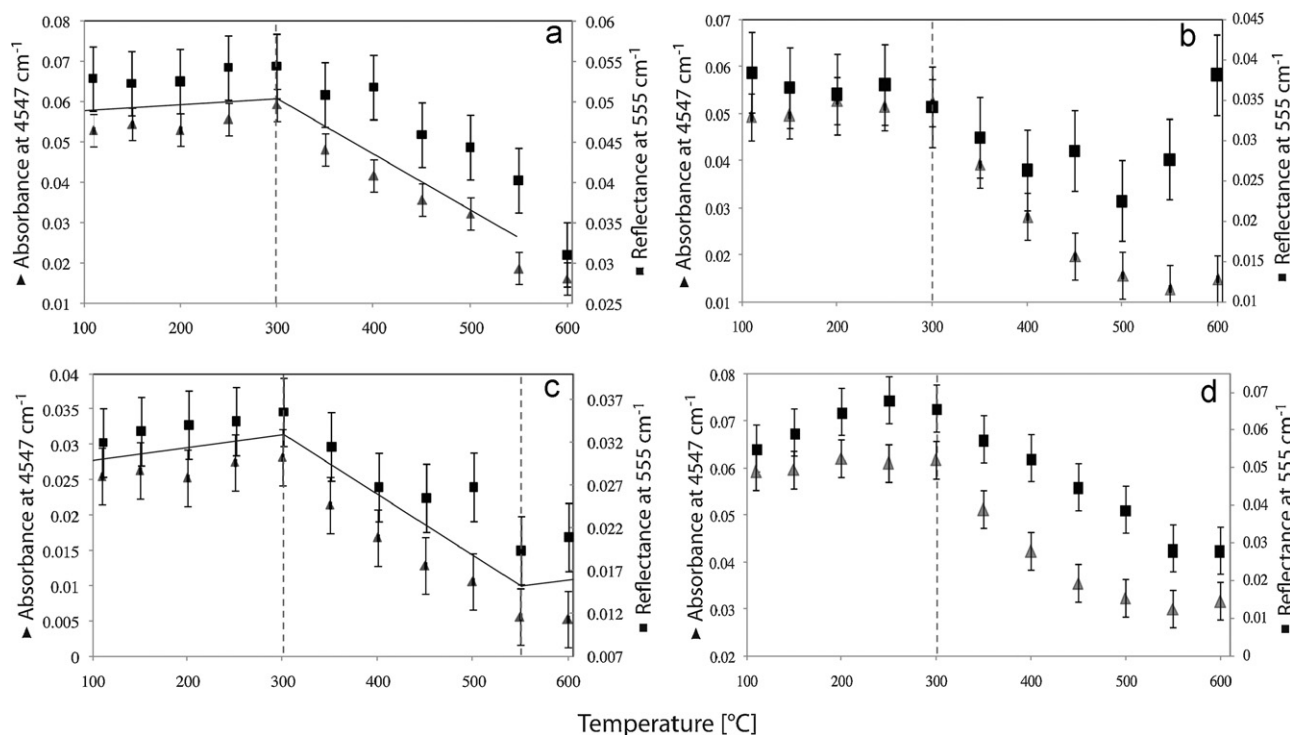
Fig. 10. Plots of the reflectivity at 555 cm^{-1} and the absorption at 4547 cm^{-1} (SiOH) of 4 flint samples. (a) PS-09-25, (b) PS-09-11, (c) PS-09-04 and (d) PS-09-13. The measurements of the absorption and the reflectivity were acquired on the same samples, directly one after the other, in their hydrated state. Scales to the left of the graphs: absorption at 4547 cm^{-1} (▲), scales to the right: reflectivity at 555 cm^{-1} (■). The starting temperature of the reduction of the two bands lies between 300 °C and 350 °C (dotted line) and the identical pace of their reduction shows their correlation.

complete annealing sequence (Fig. 9b). The remaining two control samples show reasonably close values.

3.2. Mid infrared

Spectra of the 11 flint samples show a band at 555 cm^{-1} as already described by Schmidt and Fröhlich [20]. Mid infrared spectra were acquired on hydrated samples. The reflectivity at 555 cm^{-1} decreases with successive annealing steps from 300 °C upwards (Fig. 10). The pace of reduction is identical with the pace of reduction of silanole in the samples (Fig. 10) indicating a strong correlation.

4. Discussion and conclusion

The 5 control samples show the experimental protocol to be representative of samples heated to a single annealing temperature. Concerning the annealing time, Fukuda and Nakashima [12] found the reduction of silanole to be most intense within the first 50 min of annealing at 550 °C. Our results confirm that there is no significant difference in the loss of SiOH between samples annealed during 3 h and 6 h.

Silanole starts to reduce from 250 to 300 °C upwards. The appearance of isolated SiOH coincides with the beginning of the loss. The concomitant beginning of silanole isolation and the reduction of its total concentration suggests that SiOH is not only involved in H-bonding with H$_2$O but also with vicinal SiOH. As already pointed out by earlier works [6–8], the majority of SiOH in flint and agate samples is lost at 550–600 °C.

The SiOH concentration in some of the flint and all agate samples seems to increase until 200–250 °C. The apparent augmentation below 200 °C can be explained by the decreasing influence of molecular water that forms hydrogen bonds with silanole groups.

As seen from the experimental (Section 3.1.2), H-bonding reduces the molar absorption coefficient of the silanole band. Thus, the enlargement of the SiOH combination band at low temperatures is likely to be caused by the liberation of silanole from H-bonded pore water.

The experiments show molecular water to be held until high temperatures as already pointed out by earlier works [6–8,12]. The concentration of H$_2$O, strongly retained in closed pores, behaves heterogeneously in different samples. Most of the samples gain water over at least a part of the studied temperature interval (Fig. 4a and c). The gain begins at 250–300 °C indicating the conversion of OH in silanole to H$_2$O. This water is held in closed pores, most likely as isolated H$_2$O molecules at twin interfaces, and cannot be evacuated. The concomitant reduction of free Si–O vibrations, as seen from the 555 cm^{-1} band [20], above 250–300 °C suggests the reaction:

$$Si–OH \ HO–Si \rightarrow Si–O–Si + H_2O \tag{1}$$
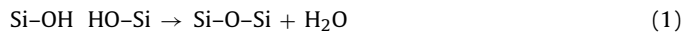
This reaction, creating new bridging Si–O–Si, was reported for annealed and hydrothermally treated chalcedony [7,21] and contributes to the closing of the open porosity of the studied samples. Plots showing the reduction of open pores indicate more intense closing from ≈300 °C upwards for some of the samples (indicated by sample PS-09-25 in Fig. 7). However, the analyses suggest that open porosity closure begins at lower temperatures. This apparent low temperature loss of open porosity might be caused by the loss of H$_2$O, evacuated from very small open pores below 250 °C and not easily reabsorbed upon rehydration of the samples. The surface of closed pores of small dimensions increases, for H$_2$O resulting from reaction (1) that cannot be evacuated through open porosity (Fig. 4a and c) needs place in the chalcedony framework. In some of the samples, newly created H$_2$O can be evacuated through open pores or fractures and the molecular water concentration, mea-

sured through the H_2O combination band, decreases continuously from 300 °C upwards (Fig. 4b). This is also the case for the studied agate samples (Fig. 4d), indicating that hydrothermally formed chalcedony contains a more open framework of pores than most of the sedimentary chalcedony, allowing an easier evacuation of H_2O. A more open porosity in hydrothermal chalcedony can also account for the continuous loss of silanole of the agate samples.

The evolution of strongly held H_2O plotted against temperature shows the moment of internal fracturing (Fig. 4c). Internal fracturing can open up closed pores at temperatures where pressure (caused by H_2O vapour) in the pores becomes critical. This fracturing causes the turning point at 450 °C in Fig. 4c. The samples that show continuous water loss also exhibit very little internal fractures indicating a more open porosity through which H_2O can be more easily evacuated.

Graetsch et al. [7] showed the diminution of the silanole combination band of chalcedony upon heat treatment but reported the band's shape to remained unchanged. This finding cannot be corroborated by the present study. Hydrogen bonding of SiOH starts to reduce at 250–300 °C in hydrated state spectra. From 300 °C to 350 °C upwards, the presence of open porosity water does not influence the shape of the SiOH combination band any more. Thus, remaining silanole involved in hydrogen bonding is not in contact with the open porosity. This may indicate that the first type of silanole to be evacuated from the samples is surface silanole at the inner walls of open pores. Hydrogen bonding is progressively reduced upon higher temperatures as seen from the $4547\,cm^{-1}/4450\,cm^{-1}$ ratio. This may be due to the loss of silanole that formed H-bonds with vicinal SiOH at crystal defects and twin interfaces.

Based on the results of the present study, we propose a 4 step model of the transformations sedimentary length-fast chalcedony undergoes upon heat treatment.

(1) The first reaction of the material is the loss of water from open porosity, starting at temperatures below 200 °C.
(2) At approximately 250–300 °C, SiOH loss and the healing of defects begin. At defect sites and twin boundaries within the quartz crystallites, molecular water is created from silanole.
(3) Between 300 °C and 450 °C, the remaining silanole is not in contact with water held in open pores any more. The surface of these open pores is further reduced. The creation of new bridging Si–O–Si bonds and the accumulation of H_2O within crystallites continue. Isolated H_2O molecules at twin boundaries and defects attract more H_2O molecules and new isolated pores, containing molecular water, form.
(4) Between 450 °C and 600 °C, the concentration of water in closed pores becomes critical and produces high pressure. As a reaction to this, the rock begins internal fracturing, permitting H_2O trapped in closed pores to be evacuated.

References

[1] S. Rios, E.K.H. Salje, S.A.T. Redfern, The European Physical Journal B 20 (2001) 75–83.
[2] A. Michel-Levy, C.P.E. Munier-Chalmas, Bulletin de la société minéralogique de France 7 (1892) 159–195.
[3] S.L. Cady, H.R. Wenk, M. Sintubin, Contributions to Mineralogy and Petrology 130 (1998) 320–335.
[4] O.W. Flörke, H. Graetsch, B. Martin, K. Roller, R. Wirth, Neues Jahrbuch für Mineralogie Abhandlungen 163 (1991) 19–42.
[5] G. Miehe, H. Graetsch, O.W. Flörke, Physics and Chemistry of Minerals 10 (1984) 197–199.
[6] O.W. Flörke, B. Köhler-Herbertz, K. Langer, I. Tönges, Contributions to Mineralogy and Petrology 80 (1982) 324–333.
[7] H. Graetsch, O.W. Flörke, G. Miehe, Physics and Chemistry of Minerals 12 (1985) 300–306.
[8] C. Frondel, American Mineralogist 67 (1982) 1248–1257.
[9] C.R. Pelto, American Journal of Science 254 (1956) 32–50.
[10] R.D. Aines, S.H. Kirby, G.R. Rossman, Physics and Chemistry of Minerals 11 (1984) 204–212.
[11] R.D. Aines, G.R. Rossman, Journal of Geophysical Research 89 (1984) 4059–4071.
[12] J. Fukuda, S. Nakashima, Journal of Mineralogical and Petrological Sciences 103 (2008) 112–115.
[13] P. Cordier, J.C. Doukhan, American Mineralogist 76 (1991) 361–369.
[14] H. Scholze, Fortschritte der Mineralogie 38 (1960) 122–123.
[15] K. Langer, O.W. Flörke, Fortschritte der Mineralogie 53 (1974) 17–51.
[16] H.A. Benesi, A.C. Jones, The Journal of Physical Chemistry 63 (1959) 179–182.
[17] J.H. Anderson jr, K.A. Wickersheim, Surface Science 2 (1964) 252–260.
[18] J.H. Anderson jr, Surface Science 3 (1965) 290–291.
[19] R.S. McDonald, The Journal of Physical Chemistry 62 (1958) 1168–1178.
[20] P. Schmidt, F. Fröhlich, Spectrochimica Acta Part A: Molecular and Biomolecular Spectroscopy 78 (2011) 1476–1481.
[21] T. Moxon, S.J.B. Reed, Mineralogical Magazine 70 (2006) 485–498.